Title

Probabilistic Liquefaction Potential Mapping of Salt Lake Valley, Utah

Authors(s)

Griffen L. Erickson, Steven F. Bartlett, Barry J. Solomon, Loren R. Anderson and Michael J. Olsen

Corresponding (first) author:

Griffen L. Erickson
122 S. Central Campus Dr., Rm. 104
Salt Lake City, Utah 84112
Phone: 801-244-4993
E-mail address: griffen.erickson@gmail.com

Submission date for review copies:

Submission date for camera-ready copy:

Probabilistic Liquefaction Potential Mapping of Salt Lake Valley, Utah

Griffen L. Erickson,[a] Steven F. Bartlett,[a] M.EERI, Barry J. Solomon[b], Loren R. Anderson, [c] Michael J. Olsen[a]

This paper discusses the methodology and creation of a probabilistic liquefaction potential map for Salt Lake Valley, Utah. The proposed method can be used for probabilistic-based hazard calculations and risk assessment by calculating the annual probability of triggering liquefaction and the return period of liquefaction for areas where sufficient geotechnical and geologic data have been gathered to support the calculations. A substantial geotechnical and geological database was collected and analyzed for Salt Lake Valley using routines written in ArcGIS®. Annual probabilities of triggering liquefaction were calculated for the mapped geological units using probabilistic liquefaction susceptibility curves (Seed et al., 2003) combined with probabilistic estimates of strong motion from the National Seismic Hazard Mapping Project (Frankel et al., 2002). Based on the results, four hazard levels were established corresponding to average return period of liquefaction: low hazard (> 2500 years), moderate hazard (1000-2500 years), high hazard (500-1000 years), and very high hazard (0-500 years). The mapping project reveals that a significant part of the central and northern Salt Lake Valley has a high to very high liquefaction hazard. The mapping project better defines the liquefaction hazard areas of Salt Lake Valley over previous mapping efforts and makes use of a fully probabilistic approach. This is the first time that a fully probabilistic approach to a regional mapping effort has been completed for Salt Lake Valley.

a) Dept. Civil and Environmental Eng., University of Utah, 122 S. Central Campus Dr. Salt Lake City, Utah 84112.
b) Utah Geological Survey, 1594 W. North Temple, P.O. Box 146100, Salt Lake City, Utah 84114-6100.
c) Dept. Civil and Environmental Eng., Utah State University, 4110 Old Main Hill, Logan, Utah 84322-4110.

INTRODUCTION

Liquefaction is a loss of shear resistance in granular soils caused by a marked increase in pore water pressure induced by cyclic loading during earthquakes. Liquefaction generally occurs in loose, saturated, cohesionless soils. In a liquefied state, the soil behaves much like a dense, viscous liquid and undergoes various types of ground deformation (e.g., flow failure, lateral spread, ground oscillation, ground settlement, and bearing capacity failure). The resulting ground failure and deformation can cause severe and costly damage that is potentially life threatening. For example, during the 1964 Alaskan earthquake, 60 percent of the estimated $500 million (1964 value) of damage was related to ground failure (Budhu et al., 1987).

Accurate and reliable liquefaction hazard maps are needed for seismically active regions to help reduce earthquake losses and aid in planning and development of earthquake-resistant communities. Salt Lake Valley is a rapidly growing urban area located near the seismically active Wasatch fault zone and other faults. Potentially liquefiable sediments (mainly Holocene and Pleistocene-age gravels, sands, silty sands and silts) have been deposited in the area by streams, rivers and lakes in a relatively deep intermountain basin (Figure 1, Table 1). The combination of earthquake hazard and potentially liquefiable sediments makes mapping projects such as this important for the seismic safety and economic development of Salt Lake Valley.

Previous liquefaction maps helped to define the extent and nature of the liquefaction hazard in Salt Lake Valley. In the 1980s, Anderson et al. (1986) delineated liquefaction potential zones using liquefaction-triggering calculations based on Standard Penetration Test (SPT) results from a relatively limited geotechnical database. More recently, Solomon et al. (2004) used HAZUS (FEMA, 1999) and the liquefaction severity index (LSI) (Youd and Perkins, 1987) implemented in HAZUS to compute LSI values for a M7.0 scenario earthquake in Salt Lake Valley. This map was based solely on geologic data and mapping and did not incorporate any subsurface geotechnical data; however, Solomon et al. (2004) recognized that the map could be improved using a geotechnical database coupled with geologic data. Most recently, Bartlett and Olsen (2005) produced a lateral spread displacement hazard map for a M7.0 scenario earthquake for northern Salt Lake Valley using a large geotechnical subsurface database consisting of results from SPT, Cone Penetrometer Tests (CPT) and shear wave velocity (V_s) measurements along with surficial geologic mapping. The subsurface geotechnical data used for this map are much more extensive than

in previous maps and updated surficial geologic mapping for the western part of Salt Lake Valley (Biek et al., 2004 and Biek, 2005) were incorporated into the analysis.

CURRENT AND PROPOSED LIQUEFACTION HAZARD MAPS FOR WASATCH FRONT URBAN COUNTIES, UTAH

Improvements in the geotechnical and geologic data for Salt Lake Valley and recent advances in probabilistic liquefaction assessment (Liao et al., 1988; Budhu et al., 1989; Hwang and Lee, 1991; Heymsfield, 1999; Marrone et al., 2003; Seed et al., 2003; Rosinski et al., 2004) and probabilistic estimates of strong motion (Frankel et al., 2002) make it possible to produce probabilistic liquefaction hazard maps on a regional basis. The liquefaction hazard mapping effort in Utah is ongoing and this paper presents a probabilistic liquefaction-triggering hazard map for Salt Lake Valley. In addition to the map developed herein, the project team plans to develop additional probabilistic and scenario earthquake hazard maps for liquefaction, lateral spread displacement, and liquefaction-induced ground settlement for the urban Wasatch Front, including Salt Lake, Utah, Davis, Weber, and Cache Counties, Utah. These probabilistic and scenario maps will be valuable tools for seismic risk assessment, loss estimation, and urban planning and development.

GEOTECHNICAL AND GEOLOGIC DATA

The geologic data for Salt Lake Valley was acquired from two main sources: a surficial geologic map of the Salt Lake City segment of the Wasatch fault zone (Personius and Scott, 1992) for the eastern side of the valley and several quadrangle maps (Biek et al., 2004 and Biek, 2005) that cover the remainder of the valley. These maps were combined to produce the geologic map of the entire valley (Figure 1) that was later used in conjunction with the hazard calculations to define the extent of each hazard zone. Table 1 summarizes the geologic map units shown on Figure 1.

The geotechnical data needed to calculate the liquefaction hazard were obtained from several different sources and screened using quality indicators developed by Bartlett and Olsen (2005). Overall there were approximately 930 SPT boreholes and 400 CPT soundings collected in the study area (Figures 2 and 3). A primary source of data was the Utah Department of Transportation, which provided a significant electronic subsurface database from the recently finished I-15 Reconstruction project. Other subsurface data sources included Salt Lake County Planning, local area consultants, and data used in the previous

liquefaction potential map by Anderson et al. (1986). The subsurface database included SPT, CPT, V_s, groundwater levels, soil descriptions, and other classification properties such as fines content and Atterberg limits.

The amount and spatial distribution of the collected data provided a reasonable characterization of most of the geologic units in the mapped area; however, some judgment was applied, as discussed in the map production section of this paper. In addition, some required information was missing in some of the SPT boreholes (e.g., soil unit weight, fines content, etc.). For these boreholes, Microsoft Visual Basic for Applications (VBA) routines were used to fill in data gaps by averaging according to soil type and geologic unit (Bartlett and Olsen, 2005). However, in no case were SPT blowcount values estimated; if this information was not available, the corresponding borehole information was not used. In addition, the depth to groundwater was estimated for some boreholes lacking this information. These estimates were made from nearby boreholes using an inverse distance squared method to interpolate groundwater elevations between boreholes. The inverse distance squared method was compared with results from kriging and spline interpolation methods and appeared to produce reasonable results (Bartlett and Olsen, 2005).

Other VBA routines also used to calculate the liquefaction hazard and complete the mapping process (Bartlett and Olsen, 2005) consisted of vertical effective stress and SPT blowcount correction routines. Before performing the liquefaction hazard calculations, soil intervals in the borehole data having a plastic index greater than 7 were identified and removed from the hazard analysis because they typically exhibit "clay-like" behavior during seismic events and, while they may generate excess pore water pressure, do not typically liquefy (Boulanger and Idriss, 2004).

PROBABILISTIC FRAMEWORK

The probabilistic liquefaction calculations combined probabilistic estimates of strong motion with probabilistic liquefaction potential curves to calculate the annual probability of liquefaction for the various geologic units in the mapped area. The United States Geological Survey (USGS) provided the seismic hazard curve information as part of the National Seismic Hazard Mapping Project and the probabilistic liquefaction potential curves were obtained from Seed et al. (2003). However, because the seismic hazard varies significantly within Salt Lake Valley, the USGS provided hazard curve information at 0.025 degree grid

spacing in the mapped domain (the seismic hazard values from the National Seismic Hazard Map website [http://eqhazmaps.usgs.gov/] were not used because these values are for a much coarser grid than was required for our purposes). For a given grid point, the USGS provided estimates of the mean annual rate of exceedance (λ) versus peak ground acceleration (PGA) for rock, similar to the curve shown in Figure 4. For each grid point, we requested estimates of λ corresponding to PGA values of 0.01, 0.05, 0.1, 0.2, 0.3, 0.4, 0.5, 0.6, 0.7, 0.8, 0.9, and 1.0 g to produce a reasonably uniform spacing of λ. In addition, for each estimate of λ, the corresponding modal earthquake magnitude (M) was also provided for use in the subsequent liquefaction analyses.

The USGS PGA values are for rock (NEHRP Site Class B) and were converted to PGA soil values for the liquefaction calculations using soil amplification factors and refinements to the soil site classifications developed by Seed et al. (1997). For Salt Lake Valley the seismic response units have already been classified according to their shear wave velocities in the upper 30 m (Ashland and McDonald, 2003); therefore the PGA soil amplification/deamplification curves developed by Seed et al. (1997) could be used directly with no modification.

The probability of liquefaction for a given soil and PGA and M value can be calculated from the probabilistic liquefaction potential curves developed by Seed et al. (2003). These curves use calculations similar to deterministic liquefaction methods given by NCEER (1997). Seed et al. (2003) calculated the probability of liquefaction as a function of cyclic stress ratio (CSR) and corrected SPT blow counts in clean sand ($N_{1,60}$) for a M7.5 earthquake and an effective vertical stress of 1.0 atm (Figure 5). CSR varies with depth and is a function of PGA, the total and effective vertical stress ratio and a stress reduction factor, r_d, which accounts for the flexibility of the soil column.

Seed et al. (2003) also produced a composite equation (Equation (1)) that takes into account fines content, vertical effective stress, and earthquake magnitudes other than M7.5 directly within the equation. Equation (1) gives the probability of liquefaction as a function of the following input variables:

$$P_L = \Phi\left(-\frac{\begin{pmatrix} N_{1,60}\cdot(1+0.004\cdot FC)-13.32\cdot\ln(CSR)- \\ 29.53\cdot\ln(M_w)-3.70\cdot\ln(\sigma'_v) \\ +0.05\cdot FC+44.97 \end{pmatrix}}{2.70}\right) \quad (1)$$

where

P_L = the probability of liquefaction expressed as a decimal value,

Φ = the standard cumulative normal distribution,

M_w = earthquake moment magnitude,

σ'_v = vertical effective stress, and

FC = fines content

The CSR value for Equation (1) is calculated from:

$$CSR = \left(\frac{a_{\max}}{g}\right)\cdot\left(\frac{\sigma_v}{\sigma'_v}\right)\cdot(r_d) \quad (2)$$

where

a_{max} = the peak horizontal ground surface acceleration,

g = the acceleration of gravity,

σ_v = total vertical stress,

σ'_v = vertical effective stress, and

r_d = stress reduction factor.

Equation (2) is similar to the "simplified" method of Seed and Idriss (1971) except that r_d is calculated differently based on Cetin and Seed's (2001) finding that the original stress reduction factor of Seed and Idriss (1971) is biased. They proposed a new r_d equation that is a function of depth (d), earthquake magnitude, intensity of shaking, and site stiffness (i.e. V_s for the upper 40 ft or 12 m) (Equations (3) through (6)).

d < 65 ft (20 m):

$$r_d = \frac{\left[1+\frac{-23.013-2.949\cdot a_{\max}+0.999\cdot M_w+0.016\cdot V^*_{s,40'}}{16.258+0.201\cdot e^{0.104\cdot(-d+0.0785\cdot V^*_{s,40'}+24.888)}}\right]}{\left[1+\frac{-23.013-2.949\cdot a_{\max}+0.999\cdot M_w+0.016\cdot V^*_{s,40'}}{16.258+0.201\cdot e^{0.104\cdot(0.0785\cdot V^*_{s,40'}+24.888)}}\right]} \pm \sigma_{\varepsilon r_d} \quad (3)$$

d ≥ 65 ft (20 m):

$$r_d = \frac{\left[1+\frac{-23.013-2.949\cdot a_{\max}+0.999\cdot M_w+0.016\cdot V^*_{s,40'}}{16.258+0.201\cdot e^{0.104\cdot(-65+0.0785\cdot V^*_{s,40'}+24.888)}}\right]}{\left[1+\frac{-23.013-2.949\cdot a_{\max}+0.999\cdot M_w+0.016\cdot V^*_{s,40'}}{16.258+0.201\cdot e^{0.104\cdot(0.0785\cdot V^*_{s,40'}+24.888)}}\right]} - 0.0014\cdot(d-65) \pm \sigma_{\varepsilon r_d} \quad (4)$$

where

$\sigma_{\varepsilon r_d}(d) = d^{0.850}\cdot 0.0072$ [for d < 40 ft or 12 m], and (5)

$\sigma_{\varepsilon r_d}(d) = 40^{0.850}\cdot 0.0072$ [for d ≥ 40 ft or 12 m]. (6)

Before Equation (1) can be used, the seismic hazard curve, which is a cumulative probability density function (CDF), must be converted to a probability density function (PDF). This was done by differencing values on the seismic hazard curve to obtain "interval probabilities" (i.e., the probability that PGA is found between the two selected PGA values). For the liquefaction calculations in Equation (1), a point estimate of PGA is required, so the midpoint of each PGA bin was used for this equation, and the corresponding interval probability and modal M value were applied in Equation (7) below to represent the annual probability of peak ground acceleration and earthquake magnitude for that acceleration.

The annual probability of liquefaction at a point can then be found by summing (i.e., aggregating):

$$P[L] = \sum_i P[L|A_i, M(A_i)]\cdot P[A_i, M(A_i)] \quad (7)$$

where

P[L] = annual probability of liquefaction,

$P[L|A_i, M(A_i)]$ = conditional probability of liquefaction given the peak ground acceleration (A_i) and the earthquake magnitude [$M(A_i)$] for that acceleration,

$P[A_i, M(A_i)]$ = annual probability of peak ground acceleration and earthquake magnitude for that acceleration, and

$M(A_i)$ = the weighted modal magnitude of the earthquakes contributing to the annual probability of A_i.

The first probability in Equation (7) is calculated from Equation (1) and is conditioned on a particular A and M pair where A is the bin midpoint value. The second probability is the internal probability corresponding to the A and M pair.

Ultimately, the final map was expressed in terms of the average return period of liquefaction instead of the annual probability of liquefaction. Equation (8) was used to convert annual liquefaction probabilities to return periods using the Poisson model, as further described in Kramer (1996). The Poisson model can be used to relate the probability of at least one liquefaction event in time t with the average return period for that event in the following way:

$$P[L] = 1 - e^{-\lambda t} \tag{8}$$

where

P[L] = annual probability of liquefaction determined from Equation (4),

t = exposure time (set equal to 1 year in order to coincide with "annual" probability of liquefaction values), and

λ = mean annual rate of exceedance.

Equation (8) was solved for λ and the average return period of liquefaction was simply taken as the inverse of λ.

MAP PRODUCTION

The probabilistic calculations and other analyses were done using routines written in the Microsoft Visual Basic for Applications (VBA) Editor in ArcGIS® for more than 930 borehole locations throughout Salt Lake Valley. The return period corresponding to the $N_{1,60}$ value having the highest probability of liquefaction was calculated at each borehole and this return period was superimposed on the surficial geologic map using ArcGIS® (Figure 6). We chose not to grid and contour the return period values because of the irregular spacing and clustering of the data. Instead, the return periods were classified and color-coded according

to the following scheme: 0-500 years (very high hazard), 500-1000 years (high hazard), 1000-2500 years (moderate hazard) and greater than 2500 years (low hazard). These return period ranges were chosen in order to coincide with existing NEHRP and building code design events (500-year and 2500-year return periods). Currently the Utah Liquefaction Advisory Group (ULAG) is developing recommendations to Salt Lake County about how to use the return period of liquefaction and building importance for hazard map implementation. In the past, Salt Lake County used a simplified version of a "decision matrix" developed with the previous mapping efforts of Anderson et al. (1986) to determine the need of geotechnical evaluations. The "special study" designations of the map show areas of relative liquefaction potential and provide a basis for requiring site-specific special studies to address liquefaction hazards. These studies can resolve uncertainties inherent in regional geological mapping and ensure safety by identifying the need for liquefaction-resistant design.

The hazard for each geologic unit was assigned using the predominant liquefaction hazard return period of the boreholes that occurred in that unit (Figure 7). However, some of the mapped units were subdivided according to hazard because there was a trend or spatial change in the hazard classification for these units. In addition, some of the units in small map areas had minimal or no borehole sampling. If the same unit occurred with data elsewhere in the valley, these additional data were used to help assign the hazard level; otherwise the geologic description, type of sediments and depositional environment (e.g., alluvial, lacustrine, deltaic, etc.) were used to assign the hazard. However, most of these undersampled geologic units are in the southwestern part of the valley where very dense and/or stiff soils are found. The nature of these soils in combination with the relatively deep groundwater table, makes this area much less susceptible to liquefaction. This area was consequently assigned a low liquefaction hazard (Figure 7).

CONCLUSIONS

Both the east and west flanks of Salt Lake Valley have a relatively long liquefaction return period (i.e., > 1000 yrs) (Figure 7). The deposits in these areas are generally older (pre-Holocene), denser, and generally have a deep groundwater table. The northwestern part of the valley near Great Salt Lake also has a low hazard. It should be noted, however, that in the northwestern part of the valley near Great Salt Lake, the soils can be highly variable with thin sand layers interbedded with finer grained Jordan River deltaic and Bonneville lacustrine

deposits. The shallow deltaic and lacustrine deposits underlie the majority of the northwestern part of the valley and are made up of predominately fine-grained soils, which are not generally susceptible to liquefaction. However, significant parts of the east-central and northeastern valley have a moderate to high or very high liquefaction hazard. This elevated hazard is due to the presence of relatively loose, saturated, cohesionless soil deposited by the Jordan River and streams from Big and Little Cottonwood Canyons (Figure 7). These sediments are more abundant on the east-central and northeastern part of the valley due to the asymmetrical tilting of the sedimentary basin producing more deposition in this area. Unfortunately, a large part of downtown Salt Lake City falls within a high to very high hazard zone due to the nature of the sediments and the proximity to the Salt Lake City segment of the Wasatch fault zone.

Our liquefaction-triggering map (Figure 7) improves and refines that produced by Anderson et al. (1986) (Figure 8). Most importantly, Figure 7 is fully probabilistic in that the probability of liquefaction from the borehole data has been aggregated with the strong motion estimates for the National Seismic Hazard Maps (Frankel et al., 2002) for all seismic events and their respective probabilities. In general, the extent of the moderate and high hazard zones has been reduced on our map, although both maps show areas of high to moderate hazard in the central and most urbanized parts of the valley. Significant differences in the hazard delineation can be attributed to several factors: (1) We used a significantly larger geotechnical and geologic database, producing a more robust characterization and better spatial description of the various geologic units and their respective hazard boundaries. (2) The methods used in the liquefaction calculations for Figure 7 were significantly different; probabilistic liquefaction susceptibility curves were not available when the previous map (Figure 8) was produced, thus deterministic curves were used to calculate when liquefaction would be triggered (Anderson et al., 1986). (3) The estimates of the strong motion for Figure 7 were gridded at a more uniform and finer spacing than those of Figure 8. (4) The hazard designations (e.g., low, moderate, high and very high) differ from those used by Anderson et al. (1986). Anderson et al. (1986) used the designations shown in Table 2, which were based on the critical PGA value required to trigger liquefaction based on deterministic calculations. The probabilities for these critical acceleration values were generalized from a probabilistic seismic hazard study (Anderson et al., 1986). In contrast, our hazard categories are based on the average return period of triggering liquefaction calculated from the annual probability of

liquefaction from the aggregation of both the seismic and liquefaction hazard. This approach is a more accepted and formal way of performing the hazard calculations.

The liquefaction mapping efforts in Utah are ongoing. In future years, similar probabilistic liquefaction-triggering maps and scenario earthquake maps will be generated for Utah, Davis, Weber, and Cache Counties, and probabilistic lateral spreading maps will also be produced.

ACKNOWLEDGMENTS

The authors thank the USGS for the funding of this effort, along with the Utah Liquefaction Advisory Group for its guidance and review of this work. We also thank Stephen Harmsen of the USGS fro providing the probabilistic strong motion estimates.

REFERENCES

Anderson, L. R., Keaton, J. R., Spitzley, J. E., and Allen, A. C., 1986. Liquefaction potential map for Salt Lake County, Utah: Utah State University Department of Civil and Environmental Engineering and Dames and Moore, unpublished final technical report prepared for the U.S. Geological Survey, National Earthquake Hazards Reduction Program Award No. 14-08-0001-19910, 48 p.; published as Utah Geological Survey Contract Report 94-9, 1994.

Ashland, F. X. and McDonald, G. N., 2003. Interim map showing shear wave velocity characteristics of engineering geological units in the Salt Lake Valley, Utah metropolitan area: Utah Geological Survey Open File Report 424, 43 p. pamphlet, scale 1:75,000, CD-ROM.

Bartlett, S. F. and Olsen, M. J., 2005. Probabilistic liquefaction potential and liquefaction induced ground failure maps for the urban Wasatch front: collaborative research with the University of Utah, Utah State University and the Utah Geological Survey, Phase I, FY2004, U.S.G.S. Award 04HQGR0026, 197 p.

Biek, R. F., Solomon, B. J., Keith, J. D., and Smith T. W., 2004. Interim geologic maps of the Copperton, Magna, and Tickville Spring Quadrangles, Salt Lake and Utah Counties, Utah: Utah Geological Survey Open-File Report 434, scale 1:24,000.

Biek, R. F., 2005. Geologic map of the Jordan Narrows Quadrangle, Salt Lake and Utah Counties, Utah: Utah Geological Survey Map 208, scale 1:24,000.

Boulanger, R. W., and Idriss, I. M., 2004. Evaluating the potential for liquefaction or cyclic failure of silts and clays, Technical Report UCD/CGM-04/01, Center for Geotechnical Modeling, University of California at Davis.

Budhu, M., Giese, R. F., and Baumgras, L., 1989. Liquefaction potential of surficial deposits in the city of Buffalo, New York, Technical Report NCEER-89-0036, National Center for Earthquake Engineering Research, Buffalo, New York.

Budhu, M., Vijayakumar, V., Giese, R.F., and Baumgras, L., 1987. Liquefaction potential for New York state: A preliminary report on sites in Manhattan and Buffalo, Technical Report NCEER-87-0009, National Center for Earthquake Engineering Research, Buffalo, New York.

Cetin, K. O., and Seed, R. B., 2001. Nonlinear shear mass participation factor (r_d) for cyclic shear stress ratio evaluation, Research Report No. UCB/GT-2000/08, University of California, Berkeley.

Dames and Moore, 1978. Final report, development of criteria for seismic risk mapping in Utah, for State of Utah Department of Natural Resources Seismic Safety Advisory Council. Unpublished report. July 20. 14 p.

FEMA, 1999. Hazus 99 Technical Manual, Federal Emergency Management Agency, Washington, D.C.

Frankel, A., Petersen, M., Mueller, C., Haller, K., Wheeler, R., Leyendecker E. V., Wesson, R., Harmsen, S., Cramer, C., Perkins, D., and Rukstales, K., 2002. Documentation for the 2002 Update of the National Seismic Hazard Maps, U.S.G.S. Open File Report 02-420.

Heymsfield, E., 1999. Probabilistic approach for determination of liquefaction potential. Journal of Energy Engineering, ASCE, Vol. 125, No. 1, April, pp. 18-33.

Hwang, H. H. M., and Lee, C. S., 1991. Probabilistic evaluation of liquefaction potential, Technical Report NCEER-91-0025, National Center for Earthquake Engineering Research, Buffalo, NY.

Kramer, S. L., 1996. Geotechnical Earthquake Engineering, 1st Ed., Prentice Hall, Upper Saddle River, New Jersey.

Liao, S. S. C., Veneziano, D., and Whitman, R. V., 1988. Regression models for evaluating liquefaction probability, Journal of Geotechnical and Environmental Engineering, ASCE, Vol. 112, No. 1, pp. 44-59.

Marrone, J., Ostadan, F., Youngs, R., and Litehiser, J., 2003. Probabilistic liquefaction hazard evaluation: Methods and Applications, Transactions of the 17th International Conference on Structural Mechanics in Reactor Technology (SmiRT 17), Prague, Czech Republic, August 17-22, 2003, Paper #M02-1.

NCEER, 1997. Proceedings of the NCEER workshop on evaluation of liquefaction resistance of soils, Technical Report NCEER-97-0022, National Center for Earthquake Engineering Research, Buffalo, New York.

Personius, S. F., and Scott, W. E., 1992. Surficial geologic map of the Salt Lake City segment and parts of adjacent segments of the Wasatch fault zone, Davis, Salt Lake, and Utah Counties, Utah: U.S. Geological Survey Miscellaneous Investigations Map I-2106, scale 1:50,000.

Rosinski, A., Knudsen, K. L., Wu, J., Seed, R. B., and Real, C. R., 2004. Development of regional liquefaction-induced deformation hazard maps, Geo-Trans 2004, Geotechnical Engineering for Transportation Projects (GSP No. 126), ASCE Conf. Proc. Vol. 154, No. 67, pp 797-806.

Seed, R. B., Cetin, K. O., Moss, R. E. S., Kammerer, A. M., Wu, J., Pestana, J. M., Riemer, M. F., Sancio, R. B., Bray, J. D., Kayen, R. E., and Faris, A., 2003. Recent advances in soil liquefaction engineering, a unified and consistent framework. University of California, Berkeley, Earthquake Engineering Research Center, Report No. EERC 2003-06, pp. 71.

Seed, R. B., Chang, S. W., Dickenson, S. E., and Bray, J. D., 1997. Site-dependent seismic response including recent strong motion data. Proc. Special Session on Earthquake Geotechnical Engineering, XIV International Conference on Soil Mechanics and Foundation Engineering, Hamburg, Germany, A. A., Balkema Publ., Sept. 6-12, pp.125-134.

Solomon, B. J., Storey, N. S., Wong, I., Silva, W., Gregor, N., Wright, D., and McDonald, G., 2004. Earthquake hazards scenario for a M7 earthquake on the Salt Lake City segment of the Wasatch fault zone, Utah Geological Survey Special Study 111DM.

Youd, T. L., and Perkins, D. M., 1987. Mapping of Liquefaction Severity Index, Journal of Geotechnical Engineering Division, American Society of Engineers, v. 118, p. 1374-1392.

Table 1. Geological units and descriptions

Name	Description	Age
Qaf1	Fan alluvium 1	Upper Holocene
Qaf2	Fan alluvium 2	Middle Holocene - Upper Pleistocene
Qafo	Older fan alluvium, undivided	Middle Pleistocene
Qafy	Younger fan alluvium, undivided	Holocene - Uppermost Pleistocene
Qal1	Stream alluvium 1	Upper Holocene
Qal2	Stream alluvium 2	Middle Holocene - Uppermost Pleistocene
Qaly	Younger stream alluvium, undivided	Holocene - Uppermost Pleistocene
Qalp	Stream alluvium related to Lake Bonneville regressive phase	Uppermost Pleistocene
Qes	Eolian sand	Holocene - Upper Pleistocene
Qf	Artificial fill	Historical
Qg	Glacial deposits	Middle - Upper Pleistocene
Qlaly	Lacustrine, marsh, and alluvial deposits, undivided	Holocene - Upper Pleistocene
Qlao	Lacustrine and alluvial deposits, undivided	Holocene - Upper Pleistocene
Qlbg	Lacustrine sand and gravel related to Lake Bonneville transgressive phase	Upper Pleistocene
Qlbm	Lacustrine clay and silt related to Lake Bonneville transgressive phase	Upper Pleistocene
Qlbpg	Lacustrine sand and gravel, undivided by Lake Bonneville phase	Upper Pleistocene
Qlbps	Lacustrine sand and silt, undivided by Lake Bonneville phase	Upper Pleistocene
Qlpg	Lacustrine sand and gravel related to Lake Bonneville regressive phase	Upper Pleistocene
Qlps	Lacustrine sand and silt related to Lake Bonneville regressive phase	Upper Pleistocene
Qly	Marsh and lacustrine deposits, undivided	Holocene - Uppermost Pleistocene
QTaf	Oldest alluvial-fan deposits	Middle Pleistocene
Rock	Bedrock	Various

Table 2. Liquefaction potential designations used by Anderson et al. (1986) (from Dames and Moore 1978)

Liquefaction Potential	Critical Acceleration	Approximate 100 year Exceedance Probability
High	< 0.13 g	> 50%
Moderate	0.13 g - 0.23 g	50 - 10%
Low	0.23 g - 0.30 g	10 - 5%
Very Low	> 0.30 g	< 5%

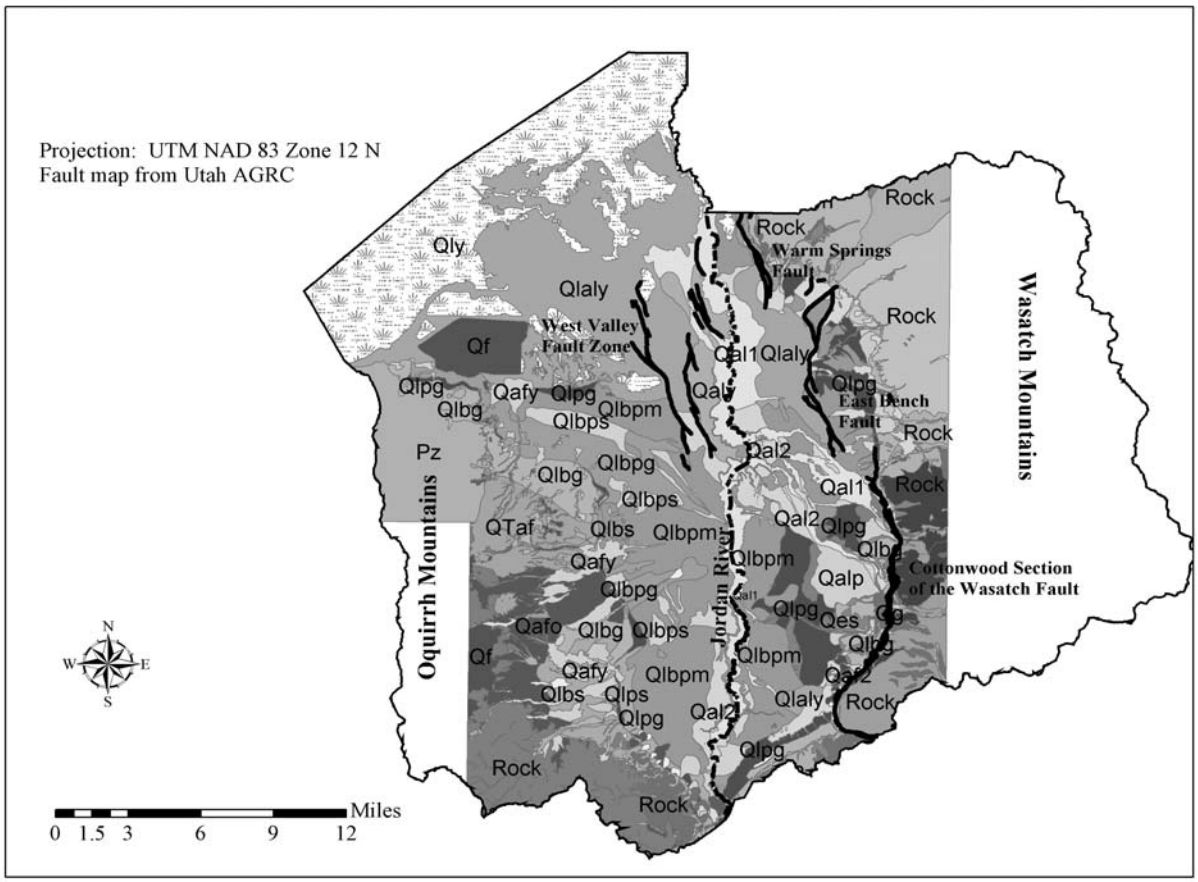

Figure 1. Surficial geologic map of Salt Lake Valley (modified from Personius and Scott, 1992; Biek et al., 2004; and Biek, 2005). Quartenary faults are shown by heavy lines; symbols for geological units are explained in Table 1.

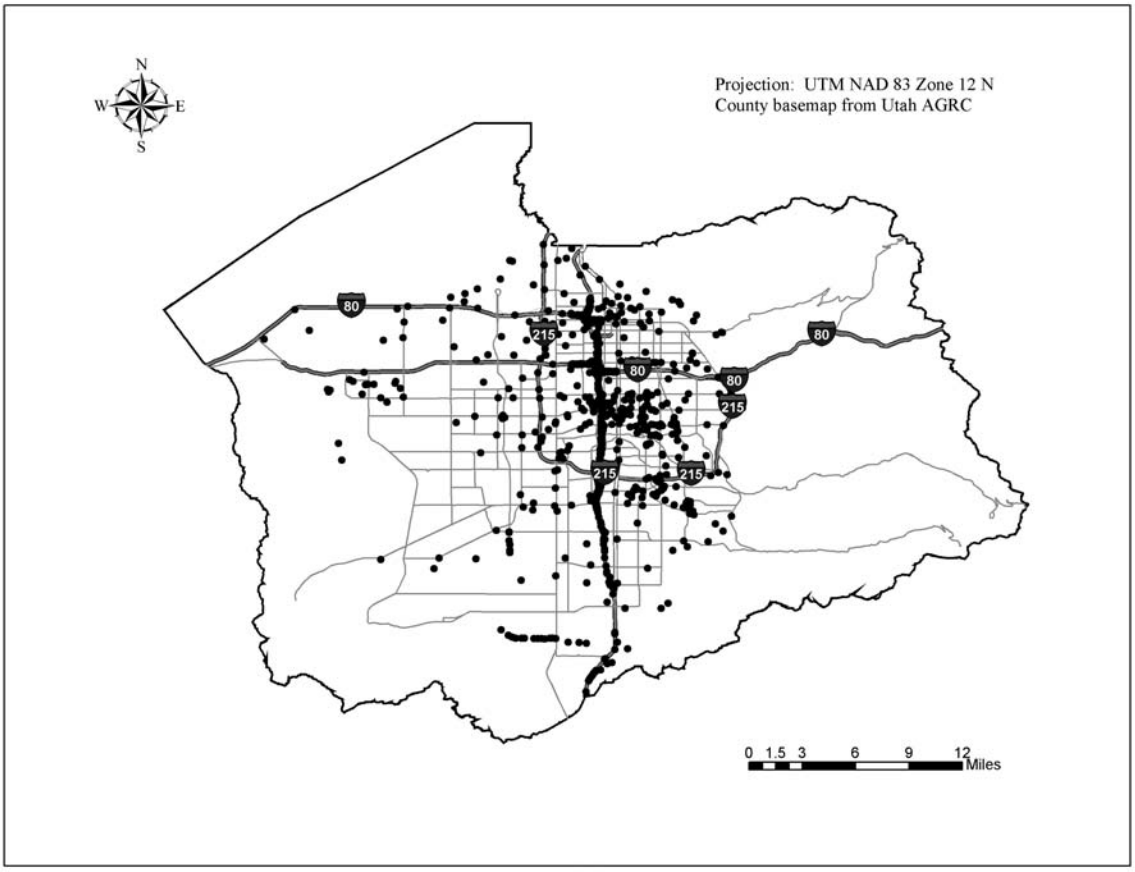

Figure 2. Standard Penetration Test data locations used for probabilistic liquefaction calculations.

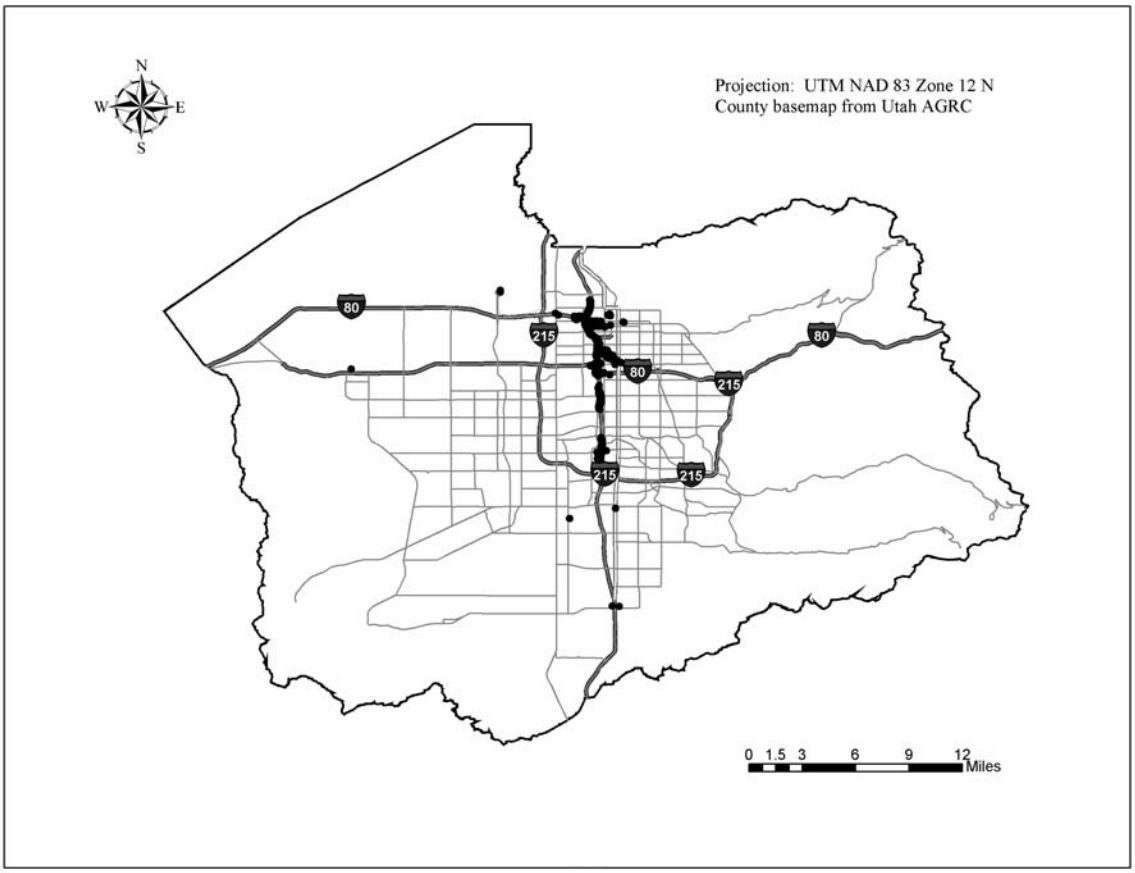

Figure 3. Cone Penotrometer Test locations in the study area.

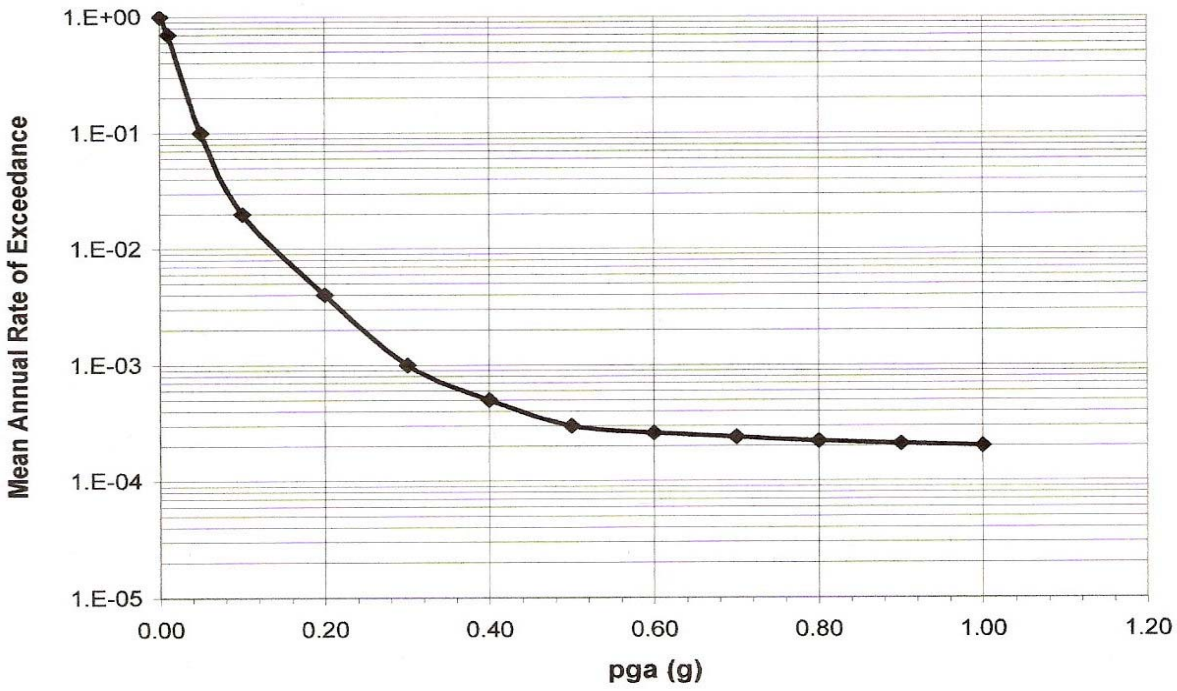

Figure 4. Example seismic hazard curve (from Bartlett and Olsen, 2005).

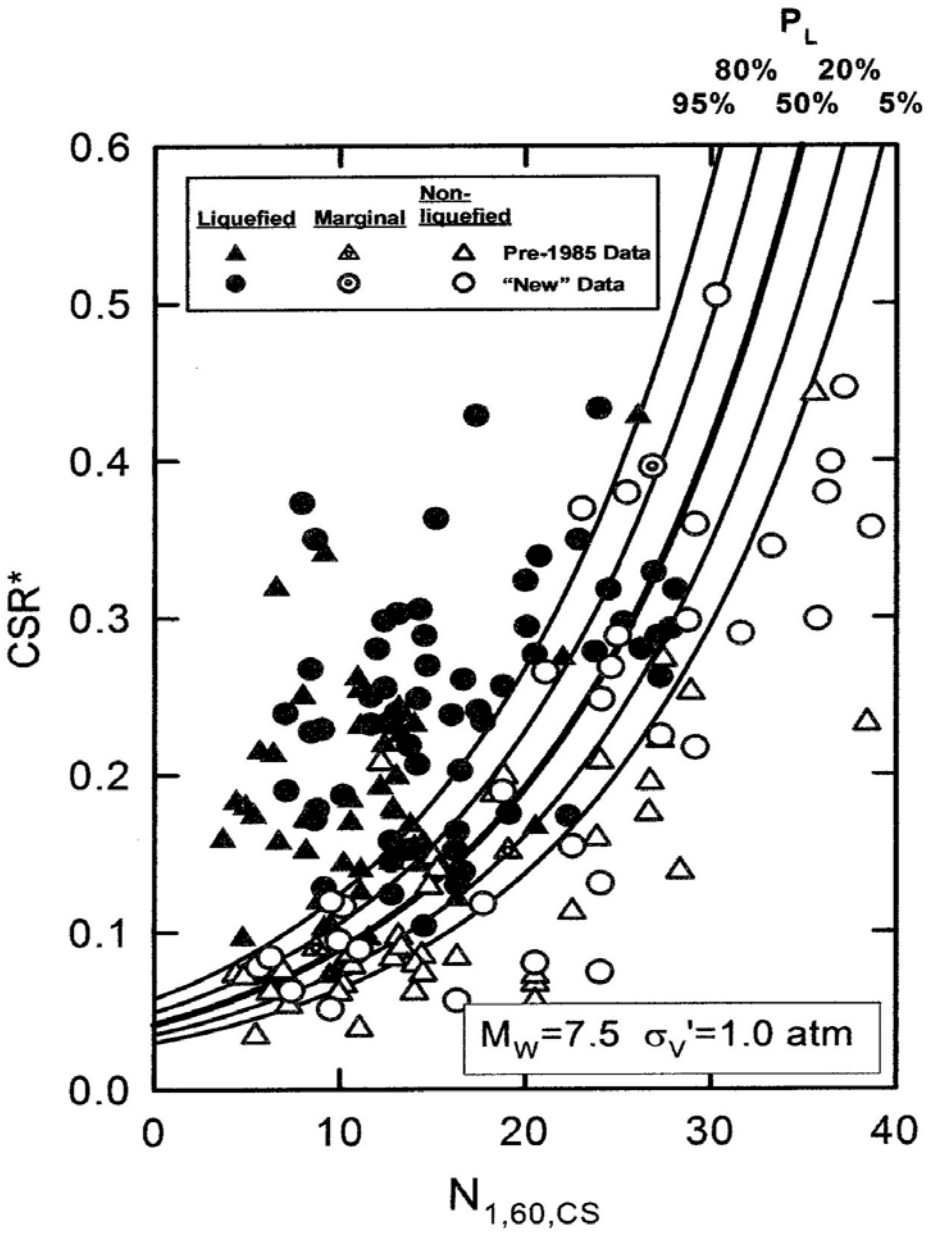

Figure 5. Liquefaction potential curves (from Seed et al., 2003). "P_L" stands for probability of liquefaction, while "CSR" stands for cyclic stress ratio.

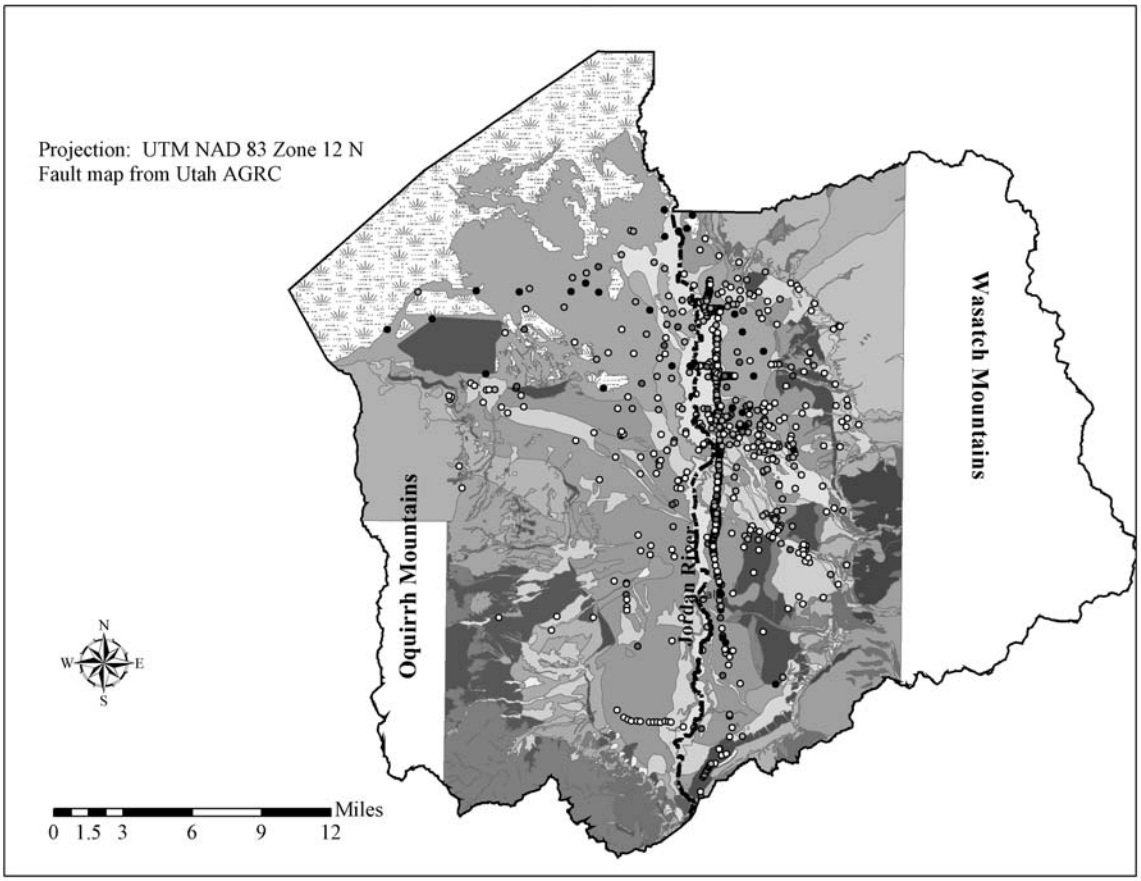

Figure 6. Plot of average liquefaction return period at borehole locations underlain by a surficial geological map (modified from Personius and Scott , 1992; Biek et al., 2004; and Biek, 2005).

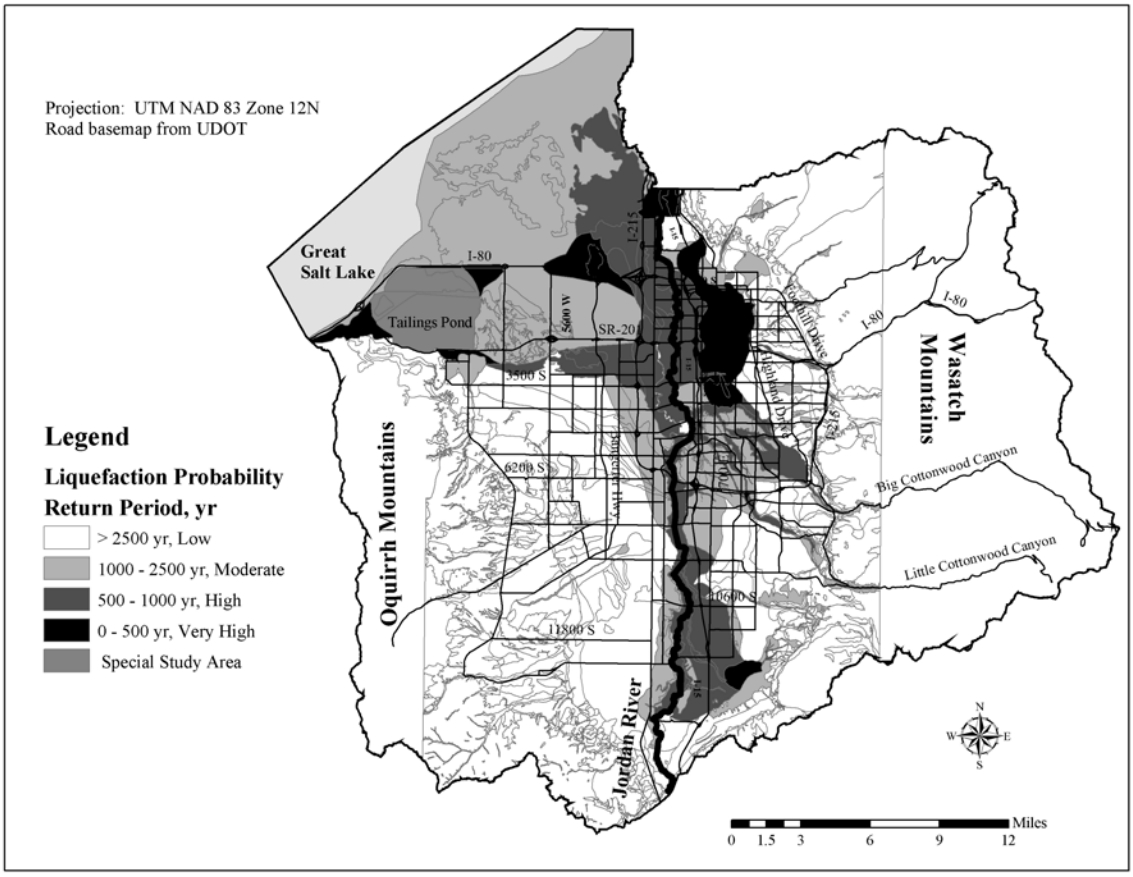

Figure 7. Probabilistic liquefaction hazard map for Salt Lake Valley, Utah.

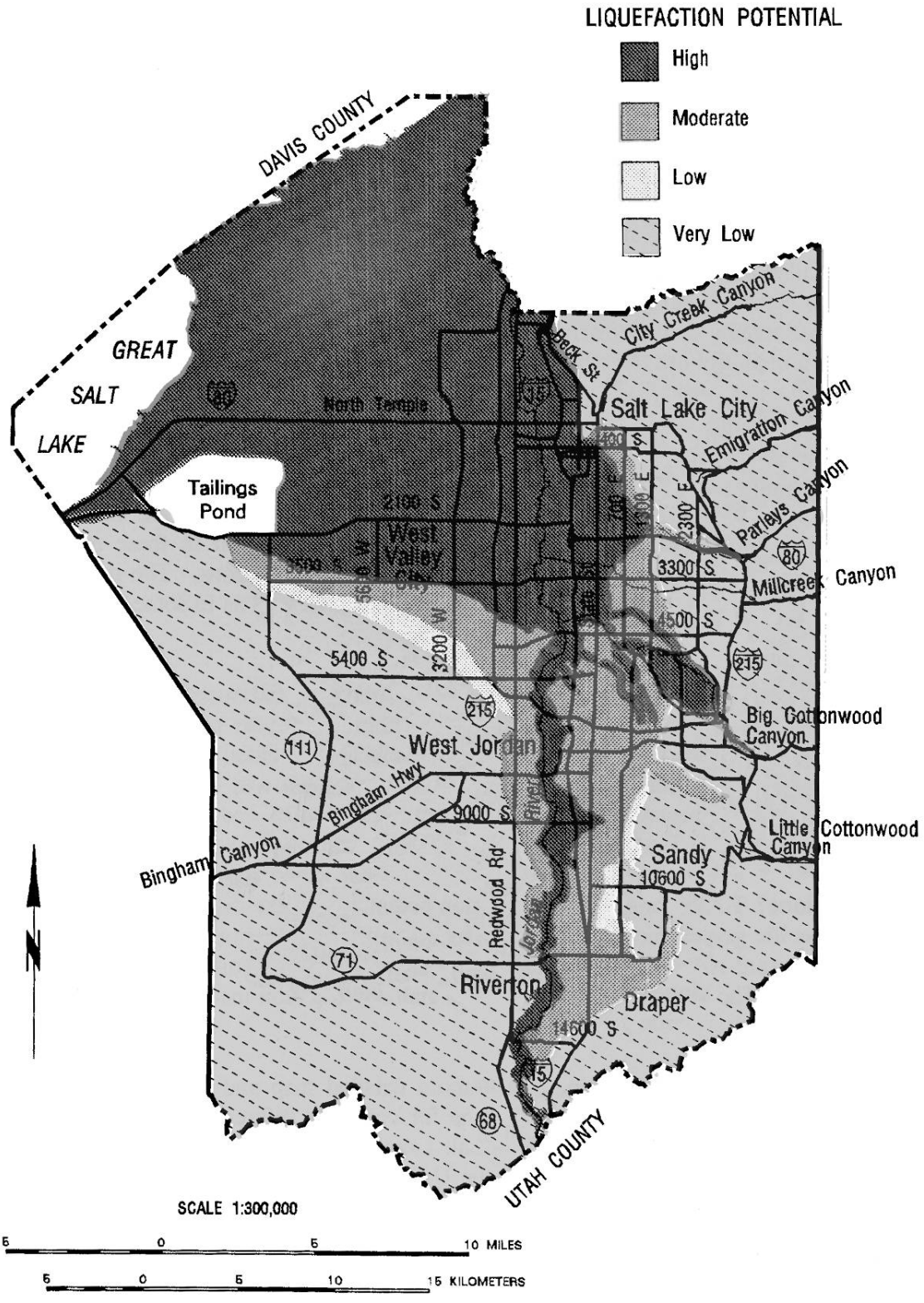

Figure 8. Liquefaction potential map for Salt Lake Valley, Utah (simplified from Anderson et al. 1986).